International Journal of Disaster Risk Reduction 17 (2016) 77–84

Contents lists available at ScienceDirect

International Journal of Disaster Risk Reduction

journal homepage: www.elsevier.com/locate/ijdrr

# Safety criteria for the trafficability of inundated roads in urban floodings

M. Kramer, K. Terheiden, S. Wieprecht *

*Institute for Modelling Hydraulic and Environmental Systems, University of Stuttgart, Germany*

ARTICLE INFO

*Article history:*
Received 2 December 2015
Received in revised form
6 April 2016
Accepted 7 April 2016
Available online 9 April 2016

*Keywords:*
Safety criteria
Trafficability
Vehicle stability
Urban flooding
Flume experiment
Prototype experiment

ABSTRACT

The probability of unexpected urban flood hazards is steadily increasing due to global warming and climate change. Consequently, there is a growing need for safety criteria determining the trafficability of inundated roads to ensure a fast and safe evacuation of people in case of such events. In order to determine those criteria, experimental investigations on the stability of two scaled watertight vehicle models and of one prototype passenger car are conducted in a laboratory flume and a steel tank.

The conducted flume experiments clearly show a dependency of vehicle stability on the flow angle, whereas the prototype experiments indicate that floating water depths are higher in prototype than in model scale, which is due to the use of a watertight vehicle model. Based on both experiments, a constant total head is proposed as decisive parameter for determining trafficability. This parameter approximates the measured stability curves and can be easily adopted in practice. Furthermore, it is in accordance with fording depths evaluated from relevant literature or by means of manufacturer inquiry. The recommended safety criteria for passenger cars and emergency vehicles are total heads of $h_E = 0.3$ m = *const.* and $h_E = 0.6$ m = *const.*, respectively.



## 1. Introduction

In the case of unexpected flood hazards such as flash floods or dam failure, the trafficability of flooded streets is a key aspect of the evacuation of urban areas and is investigated within the framework of the research project "EvaSim" (*Eva*cuation *Sim*ulation). With the aim of providing an effective and holistic approach for the development of evacuation plans in case of urban flooding events, hydrologic, hydrodynamic and traffic models are coupled. Furthermore, safety criteria concerning the trafficability of inundated streets represent the linkage between hydraulic and traffic models and therefore deliver a key parameter in flood event management.

In the present study, experimental investigations on vehicle stability and incipient velocity are undertaken. A distinction between *stability* and *roadworthiness* of vehicles is proposed for the definition of safety criteria concerning the trafficibility. Vehicle stability comprises stability in terms of floating and sliding, whereas the roadworthiness of vehicles takes additional parameters into account such as the height of air inlets or the tightness of electrical devices.

### 1.1. Instability mechanisms

In the past, two main hydrodynamic instability mechanisms, comprising floating and sliding, have been identified. Floating occurs as soon as the upward buoyancy force exceeds the downward directed submerged weight force of the vehicle. Sliding occurs when the horizontal force on the car is larger than the horizontal counteracting force, which is dependent on vehicle mass, buoyancy and the friction between vehicle tyres and road surface [1]. Both mechanisms are illustrated in Figs. 1 and 2.

### 1.2. Incipient velocity

When a vehicle is exposed to water flow, different forces act simultaneously on the partially submerged body of the car. Within the following equations, it is assumed that the exposed vehicle is not moving and has locked tyres. The acting forces include buoyancy force $F_B$, drag force $F_D$, weight force $F_G$ and friction force $F_R$. The buoyancy force is given by:

$$F_B = \rho g V \tag{1}$$

where $\rho$ is the water density, $g$ the gravitational acceleration and $V$ the immersed volume. The drag force acts on the vehicle body due to the relative motion of the vehicle with respect to the surrounding water and can be described with the following equation:

* Corresponding author.
*E-mail address:* silke.wieprecht@iws.uni-stuttgart.de (S. Wieprecht).
*URL:* http://www.iws.uni-stuttgart.de (S. Wieprecht).

http://dx.doi.org/10.1016/j.ijdrr.2016.04.003
2212-4209/

**Nomenclature**

| | |
|---|---|
| $\alpha$ | flow angle [deg] |
| $A$ | cross sectional area [$m^2$] |
| $\beta$ | inclination angle of the tilting flume [deg] |
| $C_D$ | drag coefficient [dimensionless] |
| $F$ | force [$N$] |
| $F_B$ | buoyancy force [$N$] |
| $F_D$ | drag force [$N$] |
| $F_G$ | weight force [$N$] |
| $F_N$ | normal force [$N$] |
| $Fr$ | Froude number [dimensionless] |
| $F_R$ | friction force [$N$] |
| $g$ | gravitational acceleration [$m/s^2$] |
| $h$ | water depth [$m$] |
| $h_f$ | fording depth [$m$] |
| $h_E$ | total head [$m$] |
| $h_{Si}$ | safety distance (road surface - water level) [$m$] |
| $L$ | length [$m$] |
| $L_r$ | length scale ratio [dimensionless] |
| $\mu$ | friction factor [dimensionless] |
| $m$ | model |
| $max$ | maximum |
| $n$ | prototype |
| $Q$ | flow rate [$m^3/s$] |
| $r$ | relative quantity = prototype/model quantity |
| $Re$ | Reynolds number [dimensionless] |
| $\rho$ | density [$kg/m^3$] |
| $t$ | time [$s$] |
| $v$ | velocity [$m/s$] |
| $V$ | immersed volume [$m^3$] |

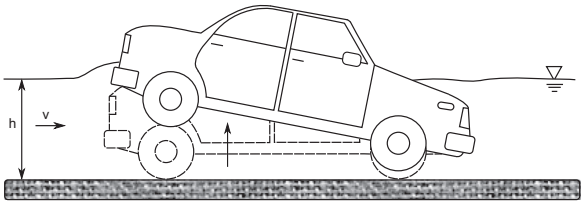


**Fig. 1.** Floating instability adopted from [1].

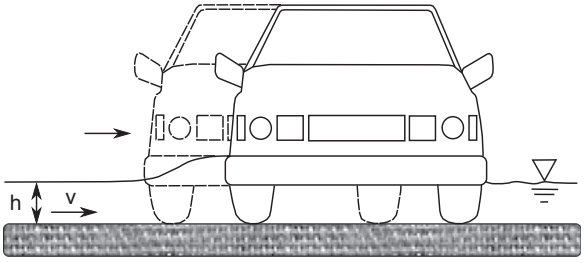


**Fig. 2.** Sliding (frictional) instability adopted from [1].

$$F_D = \frac{1}{2}\rho C_D A v^2 \tag{2}$$

where $F_D$ is the drag force, $\rho$ the density of the fluid, $A$ the cross sectional area, $C_D$ the drag coefficient and $v$ the flow velocity. According to Keller and Mitsch [2], the drag coefficient is a function of the flow depth and can be set to 1.1 once the water level is below the chassis and to 1.15 while the water level is above it. The friction force acts between the tyres and the road surface and is given by:

$$F_R = \mu F_N = \mu(F_G - F_B) \tag{3}$$

where $F_R$ is the friction force, $F_N$ the normal force, $F_G$ the weight force, $F_B$ the buoyancy force and $\mu$ the friction factor. Based on previous experimental investigations, Bonham and Hattersley set the friction factor to $\mu = 0.3$, which is almost certainly adequate for most surfaces [3]. Considering the resultant horizontal forces on the submerged vehicle body, incipient motion occurs as soon as the threshold:

$$F_D = F_R \tag{4}$$

is exceeded. Substitution of $F_D$ and $F_R$ by Eqs. (2) and (3) leads to the following equation of the incipient velocity for partially submerged vehicles in floodwater:

$$v = \sqrt{2\frac{(F_G - F_B)\mu}{\rho C_D A}} \tag{5}$$

This equation is published in different studies including Keller and Mitsch [2], where the axle load distribution of front and rear axis are taken into consideration, and Shu et al. [4], where additional experimentally determined parameters related to vehicle shape, tyre type and roughness of the road surface are considered.

### 1.3. Experimental investigations

There have been limited publications of experimental studies on vehicle stability, see Table 1. These studies differ in various aspects, e.g. in vehicle type, vehicle orientation, friction coefficient and submergence (partial and full).

Bonham and Hattersley [3] conduct tests on a partially submerged Ford Falcon model with a length scale ratio of $L_r = 25$ in order to establish criteria for the safe design of submersible causeways for use on country roads. 46 different combinations with typical flow depths ranging from $h_n = 0.11$–$0.57$ m and typical velocities between $v_n = 0.48$ m/s and 3.09 m/s are investigated in an experimental flume, where the vehicle is aligned perpendicular to the flow. This direction is defined as a flow angle of $\alpha = 90°$ within this study.

Gordon and Stone [5] carry out stability investigations on a partially submerged Morris Mini model with a length scale ratio of $L_r = 16$. The model faces upstream ($\alpha = 0°$) during the tests while vertical and horizontal reactions are measured by a modified standard beam balance. Stability curves for a car having front and rear wheels locked are obtained as a function of water depth and velocity.

Xia et al. [6] derive an equation of incipient velocity for fully submerged vehicles based on the mechanical theory of sliding

**Table 1**
Experimental studies on vehicle stability; n.d.: not defined.

| Name | Year | $L_r$ | $\mu$ | $\alpha$ | submergence |
|---|---|---|---|---|---|
| Bonham and Hattersley | 1967 | 25 | 0.3 | 90° | partial |
| Gordon and Stone | 1973 | 16 | 0.3 ÷ 1.0 | 0° | partial |
| Xia et al. | 2010 | 18, 43 | n.d. | 180° | full |
| Shu et al. | 2011 | 18 | 0.39, 0.5, 0.68 | 0°, 180° | partial |
| Teo et al. | 2012 | 18, 43 | n.d. | various | full |
| Xia et al. | 2014 | 14, 24 | 0.25, 0.75 | 0°, 90°, 180° | partial |

equilibrium. To determine empirical parameters and to validate the equation, flume experiments are conducted using die-cast model vehicles in scale ratios of $L_r = 18$ and 43, oriented with rear side facing the flow ($\alpha = 180°$). The validated equation is applied to the three types of prototype vehicles and stability curves are calculated. However, the assumption that the inside space of the prototype can be filled quickly by floodwaters may lead to an overestimation of the corresponding water depth.

Shu et al. [4] derive an equation of incipient velocity for partially submerged vehicles, which is comparable to Eq. (5) and based on the equation of Keller and Mitsch [2]. Flume tests are conducted using three types of die-cast model vehicles facing the flow with the front and the rear end of the vehicle and having a scale ratio of $L_r = 18$. The obtained test data, which indicate no substantial difference concerning vehicle orientation, are used to determine empirical parameters of the equation. These parameters are related to vehicle shape, tyre type and roughness of the road surface.

Teo et al. [7] expand the investigations of fully submerged vehicles by investigating different flow angles and ground surface gradients on vehicle models with scale ratios of $L_r = 18$ and 43. The results of this study show that the condition where the flow faces the side of the vehicle (e.g. $\alpha = 45°$) is most critical as a first trigger of stability. Furthermore, as the surface slope increases, water depth decreases and flow velocity increases at the point of vehicle instability.

citetXia2014 give an equation for the incipient velocity for partially submerged vehicles under different orientation angles. The derivation of the equation follows Xia et al. [6], but uses the reasonable assumption that a vehicle is not filled with floodwater at the initial stage of a flood event. However, the equation requires additional fitting parameters, which have to be determined throughout experimental investigations. In the study of Xia et al. [8], flume experiments on two scaled vehicle models of a Honda Accord and an Audi Q7 are undertaken and stability curves are presented for both vehicles. Furthermore, the effect of different ground slopes on incipient motion was investigated with the result of the vehicles being less stable on sloping ground.

### 1.4. Guideline values

In the past, different limits for vehicle stability have been recommended. A frequently used stability parameter is the product of water depth and water velocity ($hv$), which has been proposed in References [1,9]. A constant total head is suggested by Ref. [10], but with no explanation for the choice of this parameter. Furthermore, limits for the maximum water depth of $h_{max} = 0.3\ m$ [11–13] and maximum velocities of $v_{max} = 2$ m/s respectively 3 m/s are given in References [11,13] and Ref. [1].

Shand et al. [1] review existing guideline values and compare them to experimental and analytical results. They conclude that the limits given in [10,13] may be extremely conservative for larger vehicles, whereas all other criteria are non-conservative at certain flow conditions. As draft criteria, Shand et al. recommend relationships of a constant product of water depth and velocity ($hv = const.$). However their report captions that vehicle stability has not yet been sufficiently researched. Further investigations are needed on e.g. buoyancy in modern cars, effect of vehicle orientation related to flow direction and stability of additional categories including commercial and emergency vehicles, for an adequate definition of safety criteria [1].

### 1.5. Fording depth

The fording or wading depth is defined as the maximum water depth, which can be forded by a vehicle without supplementary equipment, and is often given in technical specifications provided by manufacturers. In comparison with passenger cars, emergency or off-road vehicles are capable of fording waters of higher depths, especially if they have a higher exhaust or a snorkel.

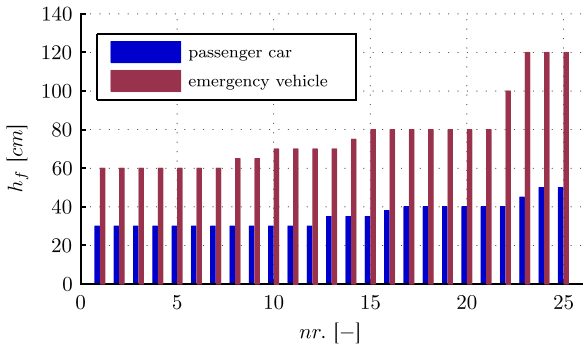


**Fig. 3.** Typical fording depths of passenger and emergency vehicles.

In the context of this study, fording depths of passenger cars and emergency vehicles are collected mainly from manufacturer's data and literature. Fig. 3 shows the fording depths, denoted as $h_f$, of 50 vehicles sorted by values. The typically used vehicles in Germany, e.g. the VW Golf passenger car or the LF 10/6 emergency vehicle are included. As result, a clear dependency of the fording depth on the type of vehicle can be observed. Typical fording depths of passenger cars range from $h_f = 30$ cm and 50 cm, while the fording depths of emergency vehicles are more wide spread from $h_f = 60$–120 cm.

Compared to safety criteria based on stability considerations, the fording depth includes parameters such as the air inlet height of the car engine, height of the car generator and ignition system, and the watertightness of electrical equipment and the interior space. These parameters exceed pure stability issues. Therefore, the fording depth can be useful when evaluating the more complex roadworthiness of vehicles passing through waters. However, as there is no clear definition of fording velocity and as vehicles usually ford at low flow velocities, the fording depth is considered a static parameter which cannot be applied to higher flow velocities.

### 1.6. Discussion

Up to now, there are limited investigations on stability analyses of vehicles on flooded streets. An analytical approach, initially founded by Keller and Mitsch [2] and later modified by Xia et al. [6,8], is based on equilibrium of forces and leads to reasonable results. However, this analytical approach requires fitting parameters, which are related to the vehicle shape, tyre type and the roughness of the road surface and have to be derived by laboratory investigations.

As existing studies mainly deal with safety criteria for passenger cars or sport utility vehicles (SUV), there is an urgent need for research into safety criteria for emergency vehicles. Especially in case of evacuation of flooded urban areas, the serviceability of emergency vehicles is of utmost importance. For vehicles, there are currently no safety criteria concerning the height of air inlets or the tightness of electrical devices. For this reason, detailed experimental investigations on the stability of two scaled models and one prototype passenger car are undertaken in a laboratory to define safety criteria for the roadworthiness of passenger cars and emergency vehicles. Manufacturer information concerning fording depths of the investigated vehicle types are evaluated, and on the basis of this information and the experiments results, new safety criteria are developed. These criteria are useful in development of evacuation plans and assist to minimize the endangerment of

civilians and emergency services persons.

## 2. Experimental investigation on vehicle stability (model scale)

For the experiments on model scale, dependent effects have to be taken into account by ensuring similarity between model and nature, implying geometrical, kinematic and dynamic similarity [14]. In free surface flows, pressure forces and viscosity effects are inferior when compared to the effects of gravity and inertia forces. Therefore, it has to be ensured that the Froude number of model and prototype experiments are equal:

$$Fr_r = \frac{v_r}{\sqrt{g_r L_r}} = 1 \tag{6}$$

where the index $r$ means relative quantity, $Fr$ is the Froude number, $v$ the velocity, $g$ the gravitational acceleration and $L$ a characteristic length. However, a major concern in hydraulic modelling based on Froude similitude are potential scale effects induced by viscous forces. To minimize those scale effects, the Reynolds number of the model ($Re_m$) has to be large enough for a turbulent flow at the smallest test flow [15]. The smallest investigated Reynolds number of the undertaken experiments is $Re_m = 4.1 \cdot 10^4$, therefore fullfilling turbulent flow conditions. $Re = \frac{v \cdot L}{\nu}$ is the Reynolds number, $v$ the velocity, $L$ the characteristic length and $\nu$ the kinematic viscosity.

### 2.1. Test flume and instrumentation

The investigations are conducted in a laboratory tilting flume with the dimensions of 20 m length, 1 m width and 0.6 m height. In order to create a unidirectional flow, flow straighteners are implemented at the flume inlet. The flow rate is measured with a magnetic inductive flow meter (E+H Promag, $\pm$ 0,5 %) located in the feeding pipe of the flume, while the water level is recorded with ultrasonic sensors (Pepperl+Fuchs UB500, $\pm$ 0,5%) mounted at several crossbars in different distances to the inlet. The mean velocity is calculated based on discharge and water level measurements at a cross-section of the flume, where undisturbed flow conditions are fulfilled.

### 2.2. Vehicle types

Two types of vehicles are utilised in the present work, see Figs. 4 and 5. Two commonly used vehicle types in Germany, a VW Golf III and the LF 10/6, which are standard passenger and emergency vehicles, are selected. The model of the VW Golf is produced by powder based laser sintering and has a length ratio of:

$$L_r = \frac{L_n}{L_m} = 9.8 \tag{7}$$

where $L_r$ is the length ratio, $L_n$ is a length in prototype scale and $L_m$ the corresponding length in model scale. The emergency vehicle model has a length ratio of $L_r = 13.1$ and the shape is based on the Ahmed body [16], while the model dimensions are chosen in accordance with the LF 10/6. The density ratio of both models is $\rho_r = 1$ and the axle load distributions of the prototype vehicles are taken into account by placing weights into the interior model spaces. As a conservative approach in terms of floating instability, the vehicles are assumed to be unladen. The specifications of the investigated models and the corresponding prototypes are given in Table 2.

To prevent water intrusion into the interior space of the vehicles, both models are designed watertight. This is in accordance with the fact that nowadays due to improvements such as dust sealing, vehicles are generally more watertight [17]. The tyres of the model vehicles are non-moving and the wet friction coefficient between tyres and ground is adjusted within preliminary investigations undertaken as part of the present work. The vehicle

**Fig. 4.** Model of the passenger car; VW Golf; $L_r = 9.8$.

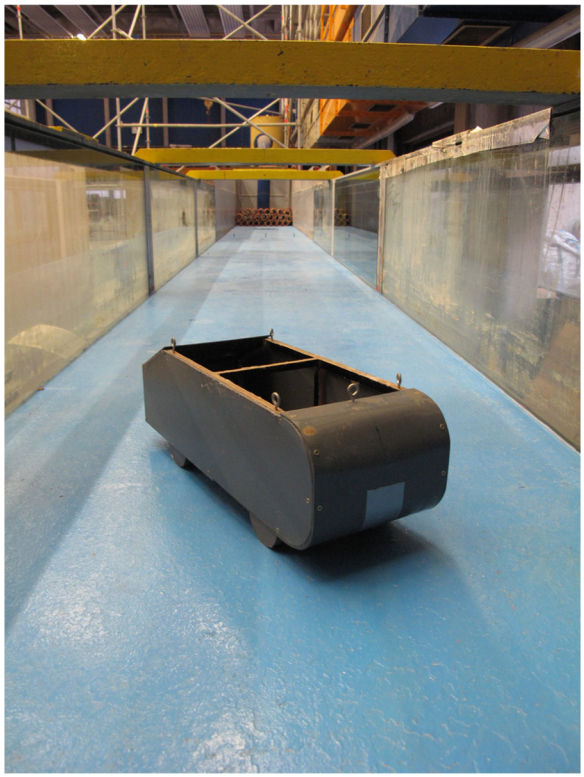

**Fig. 5.** Model of the emergency vehicle; Ahmed body; $L_r = 13.1$.

**Table 2**
Data of the investigated vehicle models and corresponding prototypes.

| Vehicle type | Length [$m$] | Height [$m$] | Width [$m$] | Empty weight [$kg$] | $L_r$ [-] |
|---|---|---|---|---|---|
| VW Golf III (Model) | 0.41 | 0.17 | 0.14 | 1.47 | 9.8 |
| VW Golf III (Prototype) | 4.02 | 1.71 | 1.41 | 1380 | 1 |
| Ahmed body (Model) | 0.52 | 0.14 | 0.19 | 2.13 | 13.1 |
| Ahmed body (Prototype) | 6.83 | 1.88 | 2.54 | 4784 | 1 |

models are placed in a steel tub which is partially filled with water. The contact conditions are realised as wetted area between tyres and steel tube and with no additional buoyancy force arising. Starting the experiment, the vehicle models are pulled with a horizontal force, which is recorded at initial vehicle movement. The wet frictional coefficient is then calculated based on the ratio of horizontal force and vehicle weight. In order to achieve a certain wet friction coefficient between tyres and ground, different material combinations are examined and a value of $\mu=0.3$ is reached, which is in accordance with Bonham and Hattersley [3].

### 2.3. Procedure

During experimental investigations, the front of the vehicles is oriented in angles of $\alpha=0°$, 45° and 90° to the flow direction. At an angle of $\alpha=0°$, the front of the vehicle is facing the flow, while at an angle of $\alpha=90°$, the vehicle is oriented perpendicular to the flow, see Fig. 6. For the detection of the beginning of instability, the flow rate is increased gradually until an initial movement of the vehicle model is observed, illustrated in Fig. 7. At that point, the vehicle model is taken out of the flume and relevant parameters such as discharge ($Q_m$), flow depth ($h_m$) and velocity ($v_m$) are recorded under stationary flow conditions. Different Froude numbers are obtained by adjusting the inclination of the tilting flume. As normal force and thus friction force decrease at increasing inclinations, the measured stability threshold may be influenced by this force reduction. However, the investigated inclination angles of the flume are between $\beta=0$ ° and 0.3° and therefore, the influence of the slope on the mentioned forces can be neglected.

### 2.4. Vehicle stability curves

Fig. 8 shows the measured stability curve of the passenger car at a flow angle of $\alpha=0$ °, converted to prototype scale. The

**Fig. 6.** Stable position; $\alpha$ = 90°.

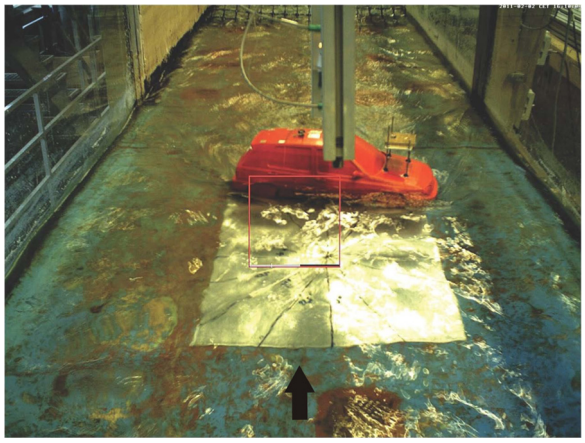

**Fig. 7.** Unstable position; $\alpha$ = 90°.

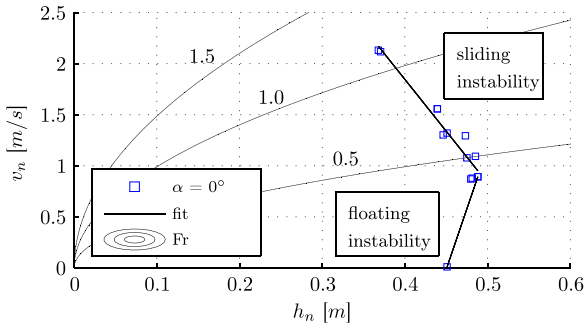


**Fig. 8.** Stability curves for the passenger car (converted to prototype scale); $\mu=0.3$; $\alpha=0°$.

incipient velocity is plotted on the ordinate against the water depth on the abscissa, while the Froude numbers are indicated as contour lines. The prototype water depths and velocities are calculated based on Froude model law:

$$h_n = L_r \cdot h_m; \quad v_n = \sqrt{L_r} \cdot v_m \tag{8}$$

where $L_r$ is the scale ratio, $h_m$ and $v_m$ are water depths and velocities in model scale and $h_n$ and $v_n$ are the corresponding parameters in prototype scale.

The results show a strong influence of the two main mechanisms (floating and sliding) on vehicle instability. At a Froude number of zero ($v_n=0$), only buoyancy force and weight force affect the vehicle body, which starts floating at a water depth of $h_n=0.45$ m. The instability remains mainly buoyancy force controlled up to Froude numbers slightly lower than $Fr=0.5$. At this point, the water depth of the stability threshold is even slightly higher than at a Froude number of zero. This is due to the fact that the water level in the proximity of the car body drops due to the flow around the partially submerged vehicle. Simultaneously, the buoyancy force decreases resulting in higher stability of the vehicle and in a higher incoming water depth compared to $Fr=0$. At Froude numbers of approx. $Fr=0.5$ and higher, the drag force is increasing and therefore, the mechanism of sliding instability is becoming more dominant. Similar behaviour is observed at flow angles of $\alpha=45°$ and 90°, represented in Fig. 9. In the area of buoyancy force controlled instability, the stability curves are almost equally independent of the flow angle. At higher Froude numbers, a spread of the stability curves is visible with the vehicle being in the most stable position at $\alpha=0°$ and most unstable position at $\alpha=45°$. However, as the shape of vehicles is typically optimized in terms of aerodynamic drag reduction, it is to be expected that the position of the vehicle with the front facing the flow is most stable. At an

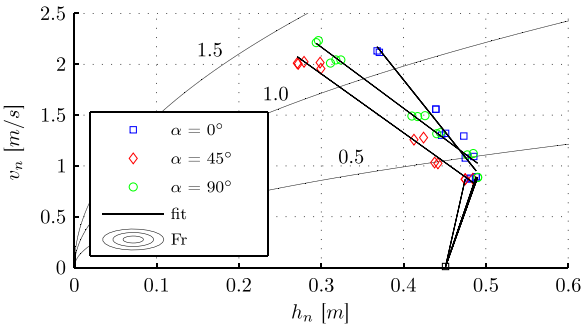


**Fig. 9.** Stability curves for the passenger car (converted to prototype scale); $\mu$=0.3; $\alpha$=0°, 45° and 90°.

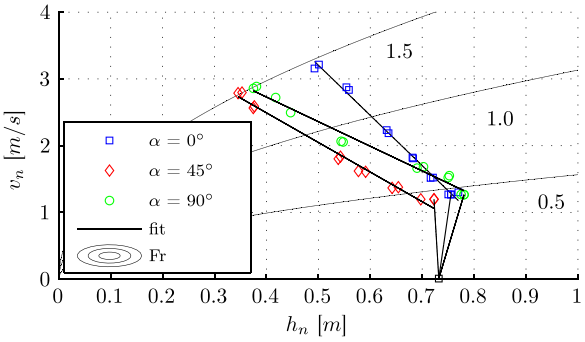


**Fig. 10.** Stability curves for the emergency car (converted to prototype scale); $\mu$=0.3; $\alpha$=0°, 45° and 90°.

angle of $\alpha$=45°, the drag force is acting on the side end of the vehicle and an incipient motion originating from this vehicle part is observed during experiments.

The stability curves for the emergency car at all investigated flow angles are presented in Fig. 10. In accordance with the Froude model law (Eq. (8)), water depths and velocities are scaled to prototype dimensions. The characteristic pattern of the stability curves is in accordance with the pattern of the passenger car. The buoyancy force is controlling the stability at low Froude numbers and therefore, the stability curves are almost independent of the flow angle within this area. At higher Froude numbers, the mechanism of sliding instability gets more dominant and the curves show a spread, depending on the particular angle between flow direction and vehicle axis being most stable at $\alpha$=0° and least stable at $\alpha$=45°. In comparison with the passenger car, the stability curves of the emergency vehicle are shifted to higher velocities and water depths. Under static conditions, the emergency car starts to float at a water depth of $h_n$=0.73 m, which is 0.28 m higher than the floating water depth of the passenger car.

## 3. Experimental investigations on floating instability (prototype scale)

### 3.1. Setup and instrumentation

For the determination of floating instability, a VW Golf III prototype having the same shape as the investigated model passenger car is mounted on a frame on the top of a steel tank. Whilst the car is no longer operable, all important technical components are present. Due to the removal of all vehicle fluids prior to experiments, the empty weight of the prototype passenger car is slightly lower than the weight of the corresponding prototype listed in Table 2. As shown in Fig. 11, the steel tank has dimensions of 6.6 m length, 4.4 m width and 2.5 m height. To detect the

**Fig. 11.** Mounting of the prototype passenger car in a laboratory steel tank.

**Fig. 12.** Detailed view of an implemented force transducer.

submerged weight of the vehicle, four force transducers (HKM SW1.4, ± 0.25%) are fixed on the wheel hubs and on the support frame, see Fig. 12. The water levels of the tank and of the inner vehicle space are recorded with ultrasonic sensors (Pepperl+Fuchs UB500, ± 0.5 %). The tank inflow is controlled with a gate valve and the flow rate is measured with a magnetic inductive flow meter (KROHNE Optiflux 2100C, ± 0.5 %).

### 3.2. Procedure

Fig. 13 shows a representative measurement of the floating instability of the prototype vehicle. At the beginning of the experiment, the water level in the tank is equal to zero, while the ultrasonic sensor in the drivers cabin indicates the height of the cabin floor (Fig. 13a). After approximately $t \approx 110$ s, the upstream gate valve is opened and a constant discharge of $Q$=50 l/s flows into the tank, see Fig. 13c. The tank water level rises during the

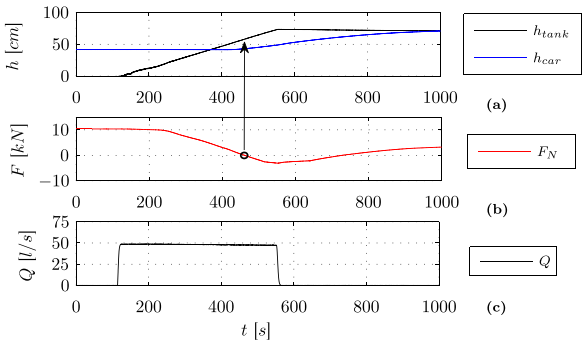


**Fig. 13.** Floating instability measurement of the prototype passenger car; (a) water depth; (b) normal force; (c) flow rate.

experiment. The drivers cabin is reached by water within a time lag of few minutes, corresponding to the horizontal distances between the black and the blue line in Fig. 13a. The measured normal force $F_N$ is shown in Fig. 13b. The buoyancy force increases with higher water levels and the vehicle becomes buoyant as the resulting normal force becomes zero. This point of instability, which is marked with a black circle in Fig. 13b, is reached at a floating depth of $h=59$ cm.

### 3.3. Experimental results

If the steel tank is slowly filled with water, more fluid is able to penetrate into the car during a certain period of time and therefore, buoyancy force decreases in comparison with faster filling procedures. The results of 11 measurements are shown in Fig. 14, where the floating depths of the prototype vehicle are plotted on the ordinate against different water rising velocities, denoted as $dh/dt$, on the abscissa. The measured floating depths are in a range of $h=0.57$ to 0.63 m. When compared to the model of the passenger car, the prototype starts to float at water depths 12–18 cm higher than predicted. One possible explanation is the difference in watertightness between the model and the prototype. As the investigated water rise velocities are relatively small compared to those during urban floodings, prototype vehicles will tend to float earlier in urban environments than indicated by the results and therefore, the assumption of watertightness seems to be reasonable concerning the determination of safety criteria.

## 4. Safety criteria

For the development of evacuation plans in case of urban flood events, the transformation of experimental results into safety criteria is essential. Existing safety criteria are derived from laboratory investigations and flood conditions, which have caused damage [13]. This is a quite reasonable approach but has deficits in theoretical background. Rather, the aim of this study is to obtain a parameter for the evaluation of the roadworthiness of vehicles in flooded urban areas, which is based on physical processes. In accordance with [10], the total (energy-) head is proposed as decisive safety criteria:

$$h_E = h + \frac{v^2}{2_g} \tag{9}$$

where $h_E$ is the total head, $h$ the water depth and $v$ the velocity. Reasons for this choice are evident:

- Under static conditions, the total head is equivalent to the fording depth. In case the total head is set to be constant, it is ensured that the water level at the stagnation point never exceeds the fording depth and therefore, technical details, such as the air inlet height of the engine, are included within the evaluation of roadworthiness.
- The shape of curve of constant total head accords well with the measured stability curves, see Figs. 10 and 11.
- The total head is a parameter which is based on physical processes rather then the commonly used product of water depth and velocity. Furthermore, the total head can be easily transferred into practice.

The determination of appropriate values is based on the experimental results as well as the evaluated fording depths of the investigated vehicles, see Fig. 12. As the lowest fording depths for passenger cars and emergency vehicles set the limit for the trafficability of flooded roads under hydrostatic conditions, these values are equal to the constant total head. Therefore, safety criteria under hydrostatic conditions are defined by $h_E=0.3$ m=*const.* and $h_E=0.6$ m=*const.* for the passenger car and the emergency vehicle, respectively. Figs. 15 and 16 show the resulting, calculated curves for the investigated vehicles including areas of low hazard, transition and high hazard. The transition area represents the difference between stability and roadworthiness and amounts $h_E=0.1$ m=*const.* for both vehicles.

As the behaviour of persons in extreme situations under stress is unforeseeable, civil traffic on inundated streets should not be allowed during urban flood events. In this context, civil traffic refers to all civilians leaving the flooded area with any type of vehicle, whereas rescue traffic describes the authorised evacuation traffic rescuing civilians (with any type of car). However, the aspect of personal behaviour under extreme conditions is not investigated in detail within the presented work, but it is considered by an overall safety distance ($h_{Si}$) between water level and road surface. The need of safety distance emerged in collaboration with hazard prevention authorities and is considered by $h_{Si}=0.5$ m. Roads within the hazard area and with a water level of 0.5 m are

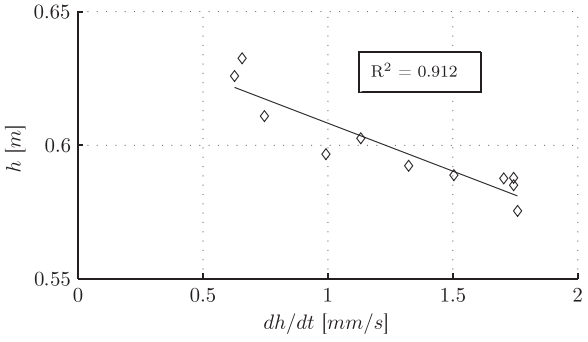


**Fig. 14.** Floating depths of the prototype passenger car at different water rising velocities.

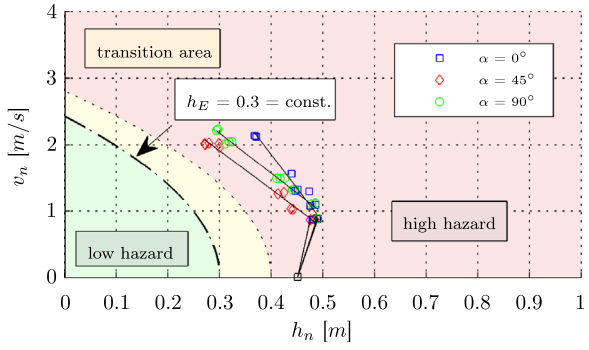


**Fig. 15.** Recommended safety criteria for the roadworthiness of passenger cars; $h_E=0.3$ m=*const.*

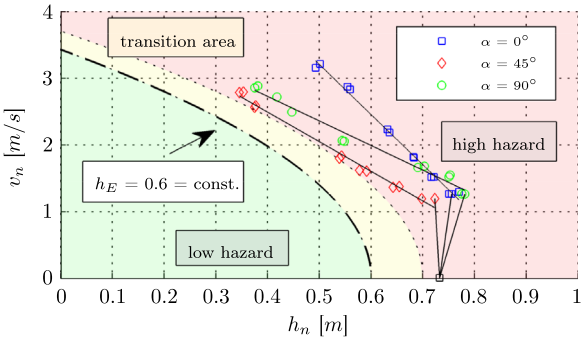


**Fig. 16.** Recommended safety criteria for the roadworthiness of emergency vehicles; $h_E$=0.6 m=*const.*

recommended to be closed for civil traffic. This recommended safety factor is chosen to avoid blockage of important evacuation routes and was derived from the dimensioning of freeboards of embankment dams in the federal state of Baden-Württemberg, Germany [18].

## 5. Conclusions and recommendations

In order to derive safety criteria for the trafficability of inundated roads during urban flood events, detailed experimental investigations on vehicle stability are conducted in a laboratory flume within this study. Two watertight vehicle models of a passenger car and an emergency vehicle are built in scale with an axle load distribution analog to the corresponding prototype. The stability of these vehicles is investigated at different inflow angles. The obtained stability curves show the same characteristic pattern for both vehicles. At low Froude numbers, the stability is controlled by buoyancy and the curves are almost independent of the flow angle. At higher Froude numbers, the sliding instability becomes more dominant, resulting in a spread of the curves with the vehicle being in the most unstable position at $\alpha$=45 °. Further investigations on the floating instability of a prototype passenger car show that the prototype starts to float at water depths which are approximately 1 to 2 dm higher than water depth being predicted from the results of the investigations with the watertight models. However, the watertightness in case of the models is a reasonable assumption concerning water rise velocities under real conditions.

Most commonly used safety criteria for the trafficability of inundated roads only consider stability aspects and therefore disregard any technical restrictions of vehicles such as the height of air inlets or the tightness of electrical devices. To specifically take these crucial restrictions into account, a constant total head is chosen as a decisive safety parameter for the roadworthiness of vehicles passing through waters. This consistent with the underlying physical processes as the total static head is equivalent to the fording depth and the curve shape of constant total head fits the measured stability data. In addition, the concept of total head can be easily transferred into practice with the following safety criteria being recommended:

- Civil traffic
  - –Safety distance: $h_{Si}$=0.5 m
- Rescue traffic
  - –Passenger car: $h_E$=0.3 m=*const.*
  - –Emergency vehicle: $h_E$=0.6 m=*const.*

## Author's contributions

Matthias Kramer and Kristina Terheiden wrote the manuscript. Matthias Kramer conducted the measurements and design of experimental setup. The data analyses and interpretation of the results were conducted by Matthias Kramer under the scientific guidance of Silke Wieprecht and Kristina Terheiden. The overall structure and scientific approval of this paper is done by Kristina Terheiden in cooperation with Silke Wieprecht. All authors contributed in the literature review, discussion and conclusion.

## Acknowledgements

This work was conducted within the cooperative research project “EvaSim”, which was funded by the German Federal Ministry of Education and Research with the reference number 13N10594.

## References

[1] T.D. Shand, R.J. Cox, M.J. Blacka, G.P. Smith, Australian rainfall and runoff, project 10: appropriate safety criteria for vehicles, Tech. Rep. ; Eng. (2011).
[2] R.J. Keller, B.F. Mitsch, Stability of cars and children in flooded streets, Int. Symp. Urban Stormwater Manag. (1992).
[3] A.J. Bonham, R.T. Hattersley. Low level causeways. Tech. Rep. 100; Water research laboratory, Manly Vale, Australia; 1967.
[4] C. Shu, J. Xia, R.A. Falconer, B. Lin, Incipient velocity for partially submerged vehicles in floodwaters, J. Hydraul. Res. 49 (6) (2011) 709–717.
[5] A.D. Gordon, P.B. Stone. Car stability on road floodways. Tech. Rep.; Water research laboratory, Manly Vale, Australia; 1973.
[6] J. Xia, F.Y. Teo, B. Lin, R.A. Falconer, Formula of incipient velocity for flooded vehicles, Nat. Hazards 58 (1) (2011) 1–14.
[7] F.Y. Teo, J. Xia, R.A. Falconer, B. Lin, Experimental studies on the interaction between vehicles and floodplain flows, Int. J. River Basin Manag. 10 (2) (2012) 149–160.
[8] J. Xia, R.A. Falconer, X. Xiao, C. Shu, Criterion of vehicle stability in floodwaters based on theoretical and experimental studies, Nat. Hazards 70 (2014) 1619–1630.
[9] D.H. Pilgrim, R.P. Canterford. Australian rainfall and runoff - a guide to flood estimation. Tech. Rep.; 1987.
[10] Guide to road design, part 5: Drainage design. Tech. Rep.; Austroads; Sydney; 2008.
[11] Floodplain development manual. Tech. Rep.; Department of Public Works, New South Wales Government, Sydney; 1986.
[12] Managing the floodplain. Tech. Rep.; Emergency Management Australia, Canberra; 1999.
[13] Floodplain development manual: the management of flood liable land. Tech. Rep.; Department of Infrastructure, Planning and Natural Resources, New South Wales Government, Sydney; 2005.
[14] H. Kobus. Hydraulic modelling. Bulletin of the German Association for Water Resources and Land Improvement (DVWK) 1984;(7).
[15] H. Chanson, The hydraulics of open channel flow: basic principles, sediment motion, hydraulic modelling, design of hydraulic structures, 2 ed., Elsevier Butterworth-Heinemann, Amsterdam, 2004.
[16] S.R. Ahmed, G. Ramm, G. Faltin. Some salient features of the time-averaged ground vehicle wave. SAE Technical Paper 840300; 1984.
[17] R.J. Cox, J.E. Ball. Stability and safety in flooded streets. Conference on Hydraulics in Civil Engineering, Hobart, Australia; 2001.
[18] Guideline on DIN 19700 for flood retention basins (in German). Tech. Rep.; Office for Environment, Measurements and Nature Conservation of the Federal State of Baden-Württemberg (LUBW); 2007.